Journal of Molecular Graphics and Modelling 40 (2013) 72–79

Contents lists available at SciVerse ScienceDirect

Journal of Molecular Graphics and Modelling

journal homepage: www.elsevier.com/locate/JMGM

Identification of potential bivalent inhibitors from natural compounds for acetylcholinesterase through *in silico* screening using multiple pharmacophores

V. Lakshmi, V. Santhosh Kannan, R. Boopathy*

Department of Biotechnology, School of Biotechnology and Genetic Engineering, Bharathiar University, Coimbatore, Tamilnadu 641046, India

ARTICLE INFO

Article history:
Received 14 March 2012
Received in revised form
30 November 2012
Accepted 17 December 2012
Available online 4 January 2013

Keywords:
Acetylcholinesterase
Catalytic site
Peripheral anionic site
Bivalent inhibitors
Virtual screening
Pharmacophore based screening

ABSTRACT

The symptomatic cure observed in the treatment of Alzheimer's disease (AD) by FDA approved drugs could possibly be due to their specificity against the active site of acetylcholinesterase (AChE) and not by targeting its pathogenicity. The AD pathogenicity involved in AChE protein is mainly due to amyloid beta peptide aggregation, which is triggered specifically by peripheral anionic site (PAS) of AChE. In the present study, a workflow has been developed for the identification and prioritization of potential compounds that could interact not only with the catalytic site but also with the PAS of AChE. To elucidate the essential structural elements of such inhibitors, pharmacophore models were constructed using PHASE, based on a set of fifteen best known AChE inhibitors. All these models on validation were further restricted to the best seven. These were transferred to PHASE database screening platform for screening 89,425 molecules deposited at the "ZINC natural product database". Novel lead molecules retrieved were subsequently subjected to molecular docking and ADME profiling. A set of 12 compounds were identified with high pharmacophore fit values and good predicted biological activity scores. These compounds not only showed higher affinity for catalytic residues, but also for Trp86 and Trp286, which are important, at PAS of AChE. The knowledge gained from this study, could lead to the discovery of potential AChE inhibitors that are highly specific for AD treatment as they are bivalent lead molecules endowed with dual binding ability for both catalytic site and PAS of AChE.

1. Introduction

The crystallographic studies on 'acetylcholinesterase-ligand' complexes provided an insight into the essential structural elements and motifs central to its catalytic function, especially on its acetylcholine (ACh) processing mechanism [1]. The striking structural feature of Acetylcholinesterase (AChE) is the presence of a narrow 20 Å deep gorge, bottom of which houses the catalytic triad residues Ser203, His447, and Glu334. The pathway lining the gorge is guarded by hydrophobic amino acid residues. The narrow entrance to this gorge is the peripheral anionic site (PAS), which comprises of aromatic residues (Tyr72, Tyr124, Trp286, and Tyr341) and Asp74. They provide the binding site for allosteric modulators/inhibitors [2,3]. In addition to its cholinergic function, AChE also acts as the target protein, in Alzheimer's disease (AD) [4].

AD is characterized by the progressive decline in cognition affecting the elderly people. One of the major therapeutic strategies for AD treatment is the catalytic intervention of AChE, which increases the level of ACh in brain. Currently, the drugs used in the treatment of AD are AChE inhibitors, such as tacrine, rivastigmine, donepezil (E2020), and galanthamine. Each drug has a differential effect on AD individuals either in delaying the neurodegeneration [5] or towards stabilization of cognitive function. However, the success of these drugs is limited by their dose-dependent hepatotoxicity and related peripheral side effects. Having implicated the peripheral anionic site of AChE in amyloid beta (Aβ) aggregation, the AD drug must potentiate the ACh level as well as/and also restrict the AChE mediated aggregation of Aβ in the brain parenchyma and cerebral microvasculature.

Invariably, inhibitors, which interact with the catalytic triad or PAS aromatic cluster, are capable of inhibiting AChE further. Several bivalent ligands (capable of binding to both catalytic site and the PAS) have been synthesized and their properties analyzed for complete inhibition of AChE. Such inhibitors are endowed with distinct conserved pharmacophore features, enabling them to establish interaction both at acylation (catalytic) site and PAS of AChE. Several attempts have been made earlier to design suitable bivalent inhibitors of AChE [6–8]. Thus the design of such inhibitors and their interaction with both catalytic site and PAS is already of potential interest in treatment of AD.

* Corresponding author. Tel.: +91 422 2428298; fax: +91 422 2422387.
E-mail addresses: boopathybiotech@gmail.com, mishlabio@gmail.com (R. Boopathy).

1093-3263/$ – see front matter © 2013 Elsevier Inc. All rights reserved.
http://dx.doi.org/10.1016/j.jmgm.2012.12.008

The AD drugs such as, tacrine and donepezil, in their protein–ligand structure has been characterized to have cation–π interactions between the protonated nitrogens and the conserved aromatic residues Trp86 and Phe337 of AChE. Moreover, π–π stacking was observed between aromatic moieties of the above ligands with aromatic amino acids of AChE [9]. Similarly additional ion–ion-interactions between the protonated nitrogens of the ligands and the anionic aspartic acid (Asp72) are also implicated in AChE–ligand binding [2]. Thus, a ligand on interaction with AChE is located at the bottom of the gorge that forms a wide hydrophobic catalytic pocket base, although larger ligands such as decamethonium and donepezil are extended to the mouth of the gorge. Having known, the mode of interaction of ligand with AChE, structure based novel drug designing using an informatics tool followed by virtual screening is attempted. It can be achieved either by (i) protein based docking or (ii) ligand based docking onto the AChE protein. In protein-based design, databases of chemical structures are exploited by docking them on to AChE. The hits are selected based upon their predicted binding energy and thus the best conformants are retrieved. In the ligand based method, pharmacophore maps are built from the ligand structures, followed by searching the chemical databases [10]. Methods combining both these tools have been found to be pivotal in search for novel candidates. PHASE [11,12] is a software tool that rapidly derives 3D chemical feature-based pharmacophore from structural data of macromolecule–ligand complexes. Pharmacophore models derived from one complex are, however, limited in terms of features represented and hence screening with multiple pharmacophore models shows great potential in the identification of new inhibitors [13,14].

In the present study, an attempt has been made to generate multiple pharmacophores, based on the crystal structures of "AChE–bivalent inhibitor complexes". A total of 15 pharmacophore models were constructed. After refining, seven of them were validated and used to screen the "ZINC-natural product database" followed by molecular docking. Prediction of ADME property for the docking simulation hits lead to the identification of novel AChE inhibitors with higher selectivity. Thus the identified bivalent AChE inhibitors are highly selective for AD treatment and may serve as lead molecules in development of drugs for AD.

2. Methodology

2.1. Pharmacophore generation

By using PHASE [11,12,14] software, 15 pharmacophore models were constructed based on AChE–ligand complexes derived from Protein Data Bank [PDB]. The excluded volumes were included for establishing more selective and restrictive pharmacophore models.

2.2. Multiple pharmacophore based screening

For validating the reliability of the 15 constructed pharmacophore models, an active set database was constructed. This database consisted of 15 ligands extracted from the complex structures discussed above [Table 1] and 83 AChE inhibitors having $IC_{50} < 100$ nm from BindingDB. The structural diversity of the data set was also taken into consideration. For validation, a decoy set was also constructed with NCI diversity set containing 1330 molecules, which are structurally diverse. The pharmacophore models were then screened against the active set for validation. The validated pharmacophores were transferred to PHASE module of Schrodinger Maestro for screening ZINC natural product database. During the database generation, the maximum number of conformers screened was set up to 400 and the remaining parameters was set as default.

2.3. Docking simulations

Glide module of Schrodinger Maestro [15–17] was used for further screening the hits (i.e. molecules) obtained through pharmacophore based search. The protonation of protein [PDB ID: 1B41] was performed with the pprep script in Glide. A grid was constructed in Glide that defined the ligand-binding site search region; the grid was defined as an enclosing box with 15 Å in all three dimensions. The standard precision (SP) docking mode was selected. The ligands in the mol2 formats were transformed into MAE format with mol2 convert utility encoded in the program and then docked flexibly into the binding site.

Autodock4 was used to perform docking simulations [18]. The protein was processed before the simulations, using the AutoDock Tools utility cofactors, water molecules were removed, polar hydrogen was added, non-polar hydrogen was merged for appropriate charge calculation, and Gasteiger charges were assigned for all the atoms in the protein. Protein and ligand atoms were converted into PDBQT format, which is the input format for AutoDock. An electrostatic grid map and a desolvation map were generated; simultaneously, affinity grid maps were also generated for each atom type in the protein and the inhibitor set. The grid boxes were centered on the active site region. In this study, Lamarckian genetic algorithm (LGA) was used for small molecule conformational search. LGA combines genetic algorithm and local search algorithm available with AutoDock4.

2.4. ADME profiling

ADME properties of the hits were calculated using Schrodinger platform. It predicts both physicochemical and pharmacokinetic properties, provides ranges for comparison with 95% of other known drugs, their reactive functional groups that may cause false positives in high-throughput screening (HTS) assays, which were eliminated. It also evaluates the acceptability of structures, based on Lipinski's rule of five, which is an essential criterion for any drug.

3. Results

3.1. Pharmacophore model generation

Pharmacophore models were generated from diverse crystal structures of "AChE–ligand complexes" which are listed in Table 1. Some of them are ligands that could interact and inhibit both through catalytic site as well as PAS. The water molecules in the crystal structure which do not participate in ligand–receptor interaction (mediated by hydrogen bonding) were deleted. The 15 pharmacophore models differ in their number of Acceptor (A), Donor (D), Hydrophobic (H), Positive (P) and Aromatic rings (R) features as shown in Table 2. Negative pharmacophore feature was not observed. Also their spatial arrangement has been represented in Fig. 1 with a common frame of reference. For example, a representative of the pharmacophore model (1EVE) as given in Fig. 1 shows six hydrophobic groups, two hydrogen-bond acceptors, three hydrogen bond donors for the inhibitor E2020 (Aricept). Similarly, 3I6M shows four hydrophobic groups, two hydrogen-bond acceptors, and one hydrogen bond donors for the inhibitor N-piperidinopropyl-galanthamine.

Table 1
List of ligands distributed in AChE protein–ligand complexes. These complexes, whose ID as appeared in Protein Data Bank (PDB) are followed. The bivalent ligand–protein complexes considered for the study are shown in bold letters.

S. no.	PDB ID	Ligand name
1	1ACJ	Tacrine
2	**1ACL**	Decamethonium ion
3	1AMN	M-(N,N,N-trimethylammonio)-2,2,2-trifluoro-1,1-dihydroxyethylbenzene
4	1AX9, 2ACK	Edrophonium ion
5	1DX6, 1QTI, 1W6R, 1W76	(-)-Galanthamine
6	**1E3Q**	4-(5-{4-[Dimethyl(prop-2-enyl)ammonio]phenyl}-3-Oxopentyl)-N,N-dimethyl-N-prop-2-enylbenzenaminium
7	1E66	3-Chloro-9-ethyl-6,7,8,9,10,11-hexahydro-7,11-methanocyclooct a[B]quinolin-12-amine
8	**1EVE**	1-benzyl-4-[(5,6-dimethoxy-1-indanon-2-yl)methyl]piperidine
9	1GPK	Huperazine A
10	1GPN	Huperazine B
11	**1H22**	(S,S)-(-)-N,N′-DI-5′-[5′,6′,7′,8′-tetrahydro-2′(1′H)-quinolynyl]-1,10-diaminodecane dihydrochloride
12	**1H23**	(S,S)-(-)-N,N′-DI-5′-[5′,6′,7′,8′-tetrahydro-2′(1′H)-quinolynyl]-1,12-diaminododecane dihydrochloride
13	1HBJ	1-[3-({[(4-amino-5-fluoro-2-methylquinolin-3-yl)methyl]thio}methyl)phenyl]-2,2,2-trifluoroethane-1,1-diol
14	1ODC	N-quinolin-4-yl-N′-(1,2,3,4-tetrahydroacridin-9-yl)octane-1,8-diamine
15	**1U65**	(4S)-4,11-diethyl-4-hydroxy-3,14-dioxo-3,4,12,14-tetrahydro-1H-pyrano[3′,4′:6,7]indolizino[1,2-b]quinolin-9-yl 1,4′-bipiperidine-1′-carboxylate
16	**1UT6**	N-9-(1′,2′,3′,4′-tetrahydroacridinyl)-1,8-diaminooctane
17	**1W4L**	Galanthamine derivative
18	**1ZGB**	(5R)-5-{[10-(1,2,3,4-tetrahydroacridin-9-ylamino)decyl]amino}-5,6,7,8-tetrahydroquinolin-2(1H)-one
19	**1ZGC**	(5S)-5-{[10-(1,2,3,4-tetrahydroacridin-9-ylamino)decyl]amino}-5,6,7,8-tetrahydroquinolin-2(1H)-one
20	**2CEK**	N-[8-(1,2,3,4-tetrahydroacridin-9-ylthio)octyl]-1,2,3,4-tetrahydroacridin-9-amine
21	**2CKM**	N,N′-DI-1,2,3,4-tetrahydroacridin-9-ylheptane-1,7-diamine
22	**2CMF**	N,N′-DI-1,2,3,4-tetrahydroacridin-9-ylpentane-1,5-diamine
23	**3I6M**	(4as,6R,8as)-3-methoxy-11-(3-piperidin-1-ylpropyl)-5,6,9,10,11,12-hexahydro-4ah-[1]benzofuro[3a,3,2-ef][2]benzazepin-6-ol
24	**3I6Z**	2-{6-[(4as,6R,8as)-6-hydroxy-3-methoxy-5,6,9,10-tetrahydro-4ah-[1]benzofuro[3a,3,2-ef][2]benzazepin-11(12H)-yl]hexyl}-1,2-benzisothiazol-3(2H)-one 1,1-dioxide

3.2. Validation of pharmacophore models

The 15 pharmacophore models constructed in this study are based on the input of bivalent ligand–AChE complexes (as shown in bold letters in Table 1). They were primarily validated for their best-fit models that can identify the most active compounds in a virtual screening process. The evaluation of these pharmacophore models were carried out by screening these models against the decoy set which consists of both AChE inhibitor complexes (a set containing 83 compounds), and NCI diversity dataset II (containing 1330 molecules). The rate of recovery of active compounds against the ranked decoy database screened by the corresponding pharmacophore model is given in Table 2. There are known actives, which satisfied multiple models. For example, known actives, which satisfied 2CMF also satisfied 2CKM but not vice versa.

Only the best models that had higher recovery rate against the known actives were further used in our study. The results demonstrated that the pharmacophore models generated from candidate ligands like 1ACL, 1EVE, 1U65, 1W4L, 1ZGC, 2CMF and 3I6Z could identify the best actives, with a recovery rate comparable to the known actives (i.e. higher than 15% in the top 5% of the ranked decoy database). In fact, the pharmacophore models like 1EVE and 2CMF could retrieve diverse actives, thus demonstrating our pharmacophore is capable of identifying compounds that have completely

Table 2
Pharmacophore's were derived using PHASE of Schrodinger. Fifteen pharmacophore models were constructed based on AChE–ligand complexes derived from PDB. The pharmacophore models are denoted by their respective PDB ID from which each is derived. The pharmacophore features included are acceptor (A), hydrogen bond donor (D), hydrophobic region (H), positive charge (P) and aromatic rings (R). The total number of hits and the actual actives recovered and their corresponding percentage actives recovered by the fifteen respective pharmacophore models are tabulated. The constructed decoy set used for screening includes 83 compounds belonging to AChE inhibitor type plus NCI diversity set containing 1330 molecules.

S. no.	PDB ID	Features of pharmacophore[a]					Total number of hits recovered	Number of actives recovered	Percentage of actives recovered (%)
		Acceptor (A)	Donor (D)	Hydrophobic (H)	Positive (P)	Aromatic rings (R)			
1.	1ACL	–	–	3	2	–	58	23	27.71
2.	1E3Q	–	–	4	2	–	54	18	21.69
3.	1EVE	2	3	6	1	1	42	14	16.87
4.	1H22	2	4	7	2	–	59	17	20.48
5.	1H23	2	4	7	1	–	44	14	16.87
6.	1U65	3	–	6	–	2	29	12	14.46
7.	1UT6	–	2	4	1	–	68	21	25.30
8.	1W4L	5	2	6		1	23	09	10.84
9.	1ZGB	1	–	8	–	3	14	03	3.61
10.	1ZGC	1	3	7	–	3	17	08	9.64
11.	2CEK	1	1	9	–	4	16	08	9.64
12.	2CKM	–	1	8	–	3	17	07	8.43
13.	2CMF	–	1	8	–	2	19	09	10.84
14.	3I6M	2	1	4	1	–	26	14	16.87
15.	3I6Z	5	2	6	–	1	27	17	20.48

[a] Negative pharmacophore feature was not observed.

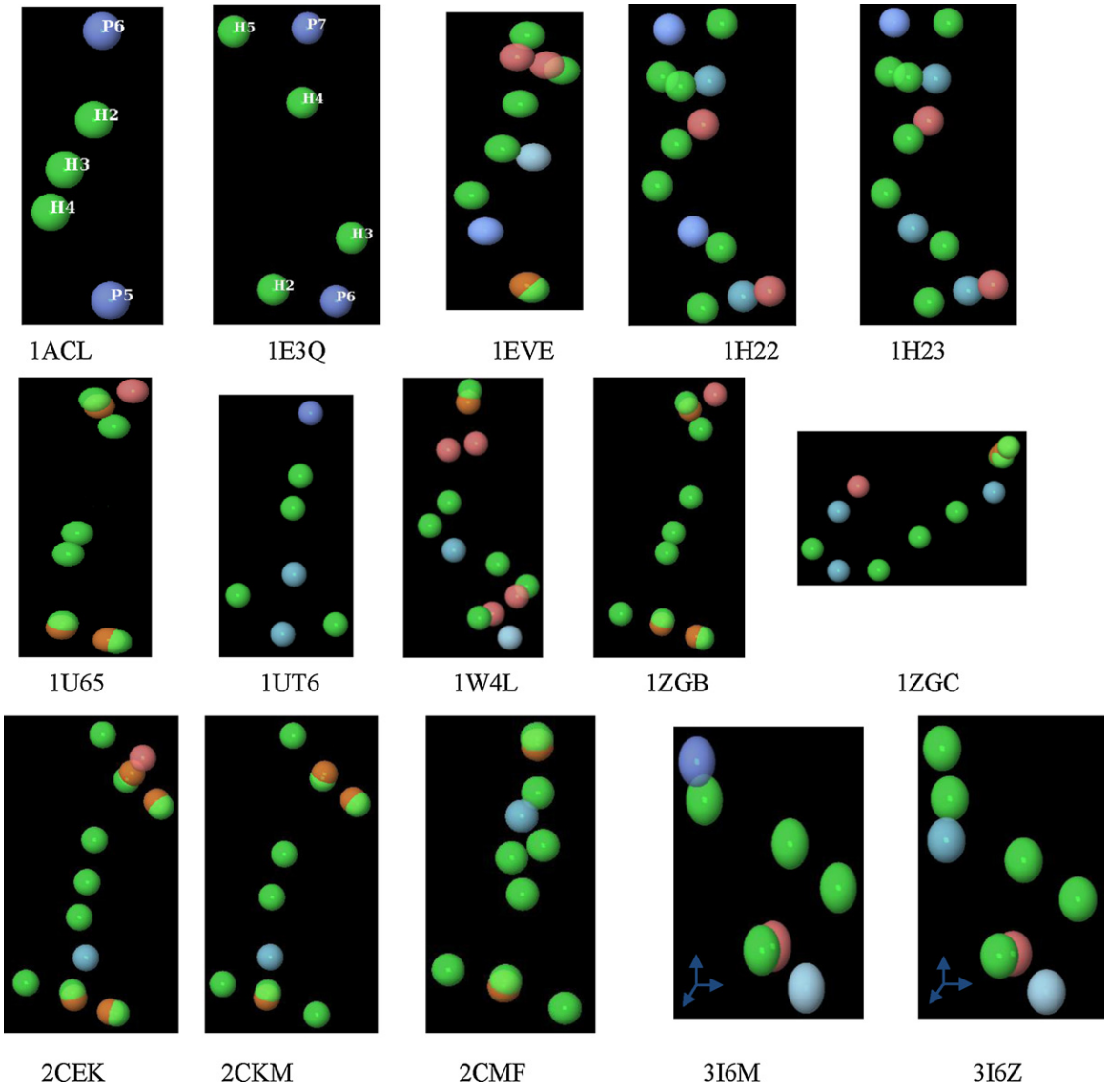

Fig. 1. Three dimensional (3D) spatial arrangement and geometric parameters of the pharmacophore model. The protocol for this model generated is as given in materials and methods. The constructed fifteen pharmacophore models are denoted by their respective PDB ID from which each is derived. The characteristic features included are acceptor (A; Light red), hydrogen bond donor (D, Light blue), hydrophobic region (H; Green), positive charge (P; Blue) and aromatic rings (R; Orange). No negative pharmacophore feature was observed.

different binding features. This phenomenon reiterates the fact that multiple pharmacophore models should be employed to identify the best possible potential hits. Although 1UT6 showed a recovery percentage of 25, it was not selected for virtual screening since it selected actives with lower affinity (micro molar range). Similarly, 3I6M could recover 26 hits but with low affinity.

3.3. Pharmacophore based virtual screening

Seven pharmacophore models which were capable of picking up top ranked actives were chosen to screen the ZINC natural product database. Table 3 shows the hits obtained against each of these pharmacophores that were validated. Some pharmacophore models were found to be very restrictive and retrieved limited hits from ZINC natural product database. For example, the pharmacophore model of 1U65 retrieved only 86 hits. In contrast, two other pharmacophore models (1ACL, 3I6Z) identified more than 600 hits. The hits obtained through pharmacophore screening were further subjected to selection, based on docking.

3.4. Docking simulations

Docking simulation of AChE (PDB Code: 1B41) and ligands was performed using the GLIDE program. The set containing 2643 compounds was further refined by deleting the compounds which were picked up by more than one pharmacophore. This resulted in a set of 1506 compounds. The binding modes for these 1506 compounds

Table 3
Total number of hits recovered from ZINC natural product database by the corresponding pharmacophore. The ZINC database included for the study consists of 89,425 molecules.

S. no.	PDB ID	No. of hits
1.	1ACL	638
2.	1EVE	239
3.	1U65	86
4.	1W4L	472
5.	1ZGC	128
6.	2CMF	354
7.	3I6Z	726

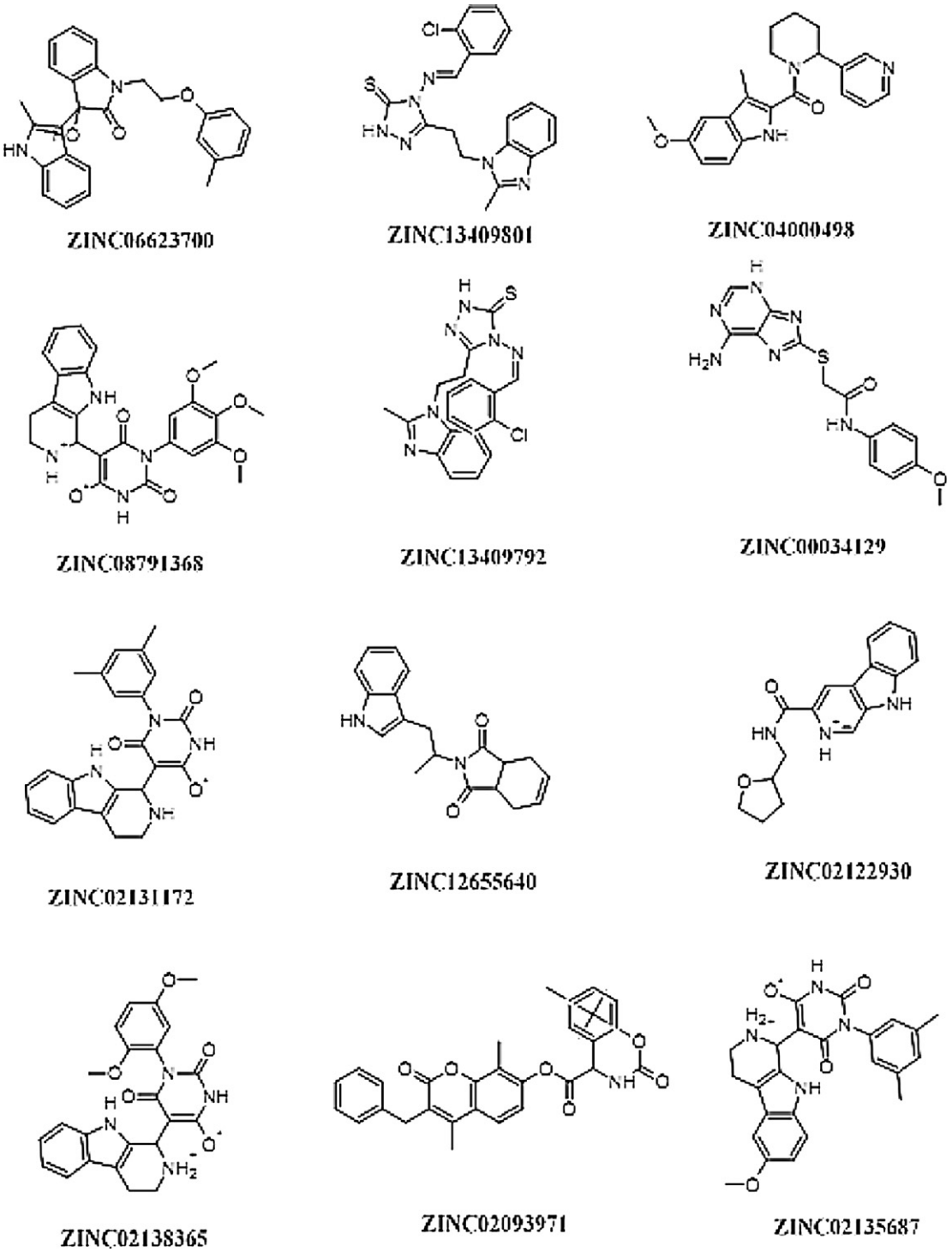

Fig. 2. Lead molecules retrieved from the ZINC natural product database as potent AChE inhibitors. These are derived by pharmacophore screening and docking combined virtual screening. The ZINC ID and their corresponding structure are given.

identified from ZINC natural product database by virtual screening were ranked according to the information obtained by glide score constraints. The first 1000 compounds exhibiting highest scores were identified from a total of 1506 compounds, which were further evaluated by docking onto the target protein using AutoDock program. After visual inspection of the top 200 compounds ranked based upon the binding energy predicted by AutoDock, the compounds with the best binding modes (exact matching of $\pi-\pi$ overlaps either with residue Trp86, or Trp286) and structural diversity were selected. Based on the Lipinski's rule of Five, knowledge of the existing AChE inhibitors and the active site requirements, 12 compounds were selected from the highest scored 200 structures. The structures of these best hits from the final screening are reported in Fig. 2. The highest scores extracted from the default scoring methods, and the predicted binding energy values for these twelve hits are summarized in Table 4. Among the hits, some were found to have novel structures when compared with already known inhibitors. The diversity of these hits demonstrated that the

Table 4
Results for the top twelve compounds from the docking studies.

S. no.	Ligand name[a]	Number of clusters	Number of conformations in the cluster	Predicted Binding energy (kcal/mol)
1.	ZINC06623700	9	7	−10.6
2.	ZINC13409801	11	5	−9.92
3.	ZINC04000498	11	7	−9.74
4.	ZINC08791368	6	8	−9.67
5.	ZINC13409792	11	5	−9.64
6.	ZINC00034129	11	5	−9.37
7.	ZINC02131172	13	5	−9.32
8.	ZINC12655640	11	6	−9.27
9.	ZINC02122930	6	11	−9.23
10.	ZINC02138365	6	9	−9.19
11.	ZINC02093971	12	7	−9
12.	ZINC02135687	13	6	−8.96

[a] Name as given in ZINC database.
Their LASSO (ligand activity in surface similarity order) score indicated high diversity (data not shown)

pharmacophore model could retrieve hits with similar features to the existing AChE inhibitors as well as novel scaffolds.

4. Discussion

Combining the best pharmacophore model based on bivalent inhibitors of AChE followed by docking, and consensus scoring function activity prediction, we could perform virtual screening onto a dataset of compounds to identify novel AChE bivalent inhibitors and to examine their important interactions for their affinity to AChE. The versatile AChE protein which, has been implicated to have multiple functions [19–21] is better understood by their 124 protein–ligand complexes reported in PDB. While the identified catalytic site is for esterase function, PAS has been documented to be involved in Aβ aggregation [22]. The pathophysiology of AD is characterized by increased Aβ aggregation together with a drastic decline in the availability of ACh. Both these phenomena are potentiated by increased PAS function and esterase activity of AChE. In fact, such functions of AChE are triggered during the onset of AD. Hence in AD patients, in order to increase the net ACh availability and to prevent Aβ aggregation, it is mandatory that both the catalytic site and PAS functions of AChE are to be simultaneously blocked.

Fig. 3 depicts the interactions of a best compound with the active site of human AChE protein. It maps out the interactions between the catalytic gorge amino acid residues (given in single letter abbreviation) of human AChE with the compound. The structure activity relationships of the best hit, against AChE observed via docking interactions showed that the oxygen and nitrogen functionalities have strong hydrogen bond interactions with active site residues Ser203, Gly122 and Tyr124. Thus, these reactive chemical entities are essential for the binding of an inhibitor to the active site. In addition, the benzyl rings of highly ranked compounds form a π–π interaction with the indole ring of Trp86; further at the peripheral anionic site (PAS), the benzyl ring of identified inhibitors form another π–π interaction with the indole ring of Trp286. Such interactions are well demonstrated in the active site of AChE for better binding with different co-crystallized AChE–ligand complexes [23–27].

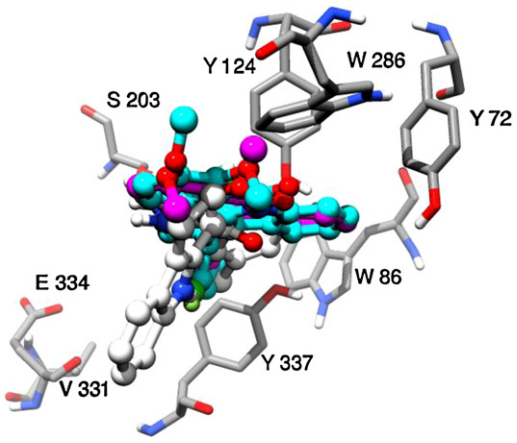

Fig. 3. The binding structures of compounds after docking into the catalytic gorge of human AChE (1B41) protein. Residues within 4 Å from the compounds are represented as wires while the ligand structures are represented in ball and stick model.

In the present study, docking of the compounds with AChE revealed that the oxygen and nitrogen functionalities of inhibitors in forming hydrogen bond with the active site residues like Tyr72, Tyr124, Tyr203 and Tyr337 amino acids of AChE is established. In the PAS, the benzyl ring forms another π–π interaction with the indole ring of Trp286. However, with certainty other identified inhibitors, despite their lack of π–π interaction with Trp86, hydrophobic interactions were also observed to play an important role in their binding to AChE (Fig. 3). Such proposed interactions of these compounds with Trp286 of AChE suggest a possibility to interfere with amyloid fibrillogenesis in addition to inhibiting the catalytic function of the enzyme. The interactions observed after docking include π–π stacking contacts with residues in the anionic substrate binding site (Trp86, Phe331, and Tyr334) and also onto the PAS (Trp286). Furthermore, these inhibitors form a hydrogen bond with amino acids at the bottom of the gorge of AChE. Such inhibitor interaction combination is also reported in the AChE crystal complex structure (e.g., donepezil, galanthamine). Therefore, the docking results enumerated in the present study predict interaction similarities for the test compounds [28–31]. In addition, although all these compounds are able to bind to the active site of the gorge, only few of them interacted with all essential residues previously identified at the binding sites of AChE.

Interestingly, the π–π interactions, hydrogen bonds, and strong hydrophobic interactions formed between these identified inhibitors, and the nearby amino acid side chains perform the dual roles, (i) to inhibit the catalytic activity of AChE by competing with ACh binding site and (ii) at the PAS (a Aβ recognition zone) for amyloid fibrillogenesis [32]. In light of the pharmacophore model developed in this study, and the knowledge gained from the *in silico* observations of the interactions between AChE and the novel inhibitors identified, it can be seen that the combination of multiple pharmacophore, molecular docking and virtual screening techniques offer a successful way of discovering an effective AChE inhibitor for further experimental studies.

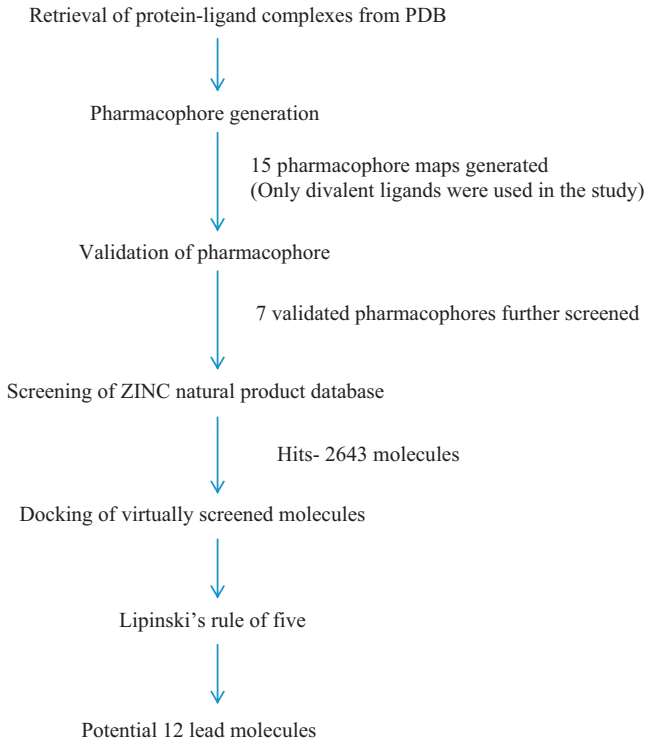

Fig. 4. Work flow of the study. The work flow chart depicts the identification of twelve potential lead molecules (shown in Fig. 2) as AChE inhibitors.

5. Conclusion

The present study [as depicted in Fig. 4] shows that a set of compounds [Table 4] along with their activities ranging over several orders can be used to generate a good pharmacophore model, which in turn can be utilized to predict the activity of a wide variety of chemical scaffolds. These models can then be used as a 3D query in database search to identify the compounds that could act as potential bivalent inhibitors of AChE. Thus the newly designed compounds based on the mapping onto the pharmacophore features and subsequent validation could be synthesized for evaluation. Those active molecules in the training set, which fits the pharmacophore model perfectly with highest scores, were further used to identify compounds from natural origin (ZINC database) followed by virtual screening. Such compounds interact with AChE through π–π stacking contacts with residues in the anionic substrate binding site (Trp86, Phe331, and Tyr334) and the PAS (Trp286). In addition, these compound s form a hydrogen bond with amino acids at the bottom of the gorge of AChE.

Thus, using a combination of pharmacophore modeling, virtual screening, and molecular docking, the putative novel bivalent AChE inhibitor(s) was identified. Such compounds which show simultaneous binding ability with the catalytic site (i.e. present in a 20 Å deep gorge) as well as PAS (i.e. onto the surface of the protein) can further be evaluated by *in vitro* and *in vivo* biological tests, for designing a drug to AD.

Acknowledgement

The Department of Biotechnology, New Delhi is thanked for funding the research and providing Research Fellowship to VSK. The authors acknowledge the suggestions provided by the reviewers which helped in improving the manuscript. Council for Scientific and Industrial Research, New Delhi and Defence Research and Development Organization-Bharathiar University Center for Life Sciences, Coimbatore is thanked for Research Fellowship to VL.

References

[1] M. Harel, I. Schalk, L. Ehret-Sabatier, F. Bouet, M. Goeldner, C. Hirth, P.H. Axelsen, I. Silman, J.L. Sussman, Quaternary ligand binding to aromatic residues in the active-site gorge of acetylcholinesterase, Proceedings of the National Academy of Sciences of the United States of America 90 (1993) 9031–9035.
[2] I. Silman, J.L. Sussman, Acetylcholinesterase: how is structure related to function? Chemico-Biological Interactions 175 (2008) 3–10.
[3] A. Ordentlich, D. Barak, C. Kronman, Y. Flashner, M. Leitner, Y. Segall, N. Ariel, S. Cohen, B. Velan, A. Shafferman, Dissection of the human acetylcholinesterase active center determinants of substrate specificity. Identification of residues constituting the anionic site, the hydrophobic site, and the acyl pocket, Journal of Biological Chemistry 268 (1993) 17083–17095.
[4] J. Munoz-Muriedas, J.M. Lopez, M. Orozco, F.J. Luque, Molecular modelling approaches to the design of acetylcholinesterase inhibitors: new challenges for the treatment of Alzheimer's disease, Current Pharmaceutical Design 10 (2004) 3131–3140.
[5] F. Mangialasche, A. Solomon, B. Winblad, P. Mecocci, M. Kivipelto, Alzheimer's disease: clinical trials and drug development, Lancet Neurol 9 (2010) 702–716.
[6] D.M. Du, P.R. Carlier, Development of bivalent acetylcholinesterase inhibitors as potential therapeutic drugs for Alzheimer's disease, Current Pharmaceutical Design 10 (2004) 3141–3156.
[7] E.H. Rydberg, B. Brumshtein, H.M. Greenblatt, D.M. Wong, D. Shaya, L.D. Williams, P.R. Carlier, Y.P. Pang, I. Silman, J.L. Sussman, Complexes of alkylene-linked tacrine dimers with Torpedo californica acetylcholinesterase: Binding of Bis5-tacrine produces a dramatic rearrangement in the active-site gorge, Journal of Medicinal Chemistry 49 (2006) 5491–5500.
[8] L.P. Orazio Nicolotti, C. Marco, L. Francesco, G. Ilenia, S. Angela, C. Angelo, Discovery of a potent and selective hetero-bivalent AChE inhibitor via bioisosteric replacement, in: Molecular Informatics Special Issue: 18th European Symposium on Quantitative Structure–Activity Relationships (EuroQSAR 2010), vol. 30, 2011, pp. 133–136.
[9] J.P. Colletier, B. Sanson, F. Nachon, E. Gabellieri, C. Fattorusso, G. Campiani, M. Weik, Conformational flexibility in the peripheral site of Torpedo californica acetylcholinesterase revealed by the complex structure with a bifunctional inhibitor, Journal of the American Chemical Society 128 (2006) 4526–4527.
[10] M.T.S.W. Patrick Walters, Mark A. Murcko, Virtual screening – an overview, Drug Discoveru Today 3 (1998) 160–178.
[11] S.L. Dixon, A.M. Smondyrev, S.N. Rao, PHASE: a novel approach to pharmacophore modeling and 3D database searching, Chemical Biology and Drug Design 67 (2006) 370–372.
[12] S.L. Dixon, A.M. Smondyrev, E.H. Knoll, S.N. Rao, D.E. Shaw, R.A. Friesner, PHASE: a new engine for pharmacophore perception, 3D QSAR model development, and 3D database screening: 1. Methodology and preliminary results, Journal of Computer-Aided Molecular Design 20 (2006) 647–671.
[13] D. Wei, X. Jiang, L. Zhou, J. Chen, Z. Chen, C. He, K. Yang, Y. Liu, J. Pei, L. Lai, Discovery of multitarget inhibitors by combining molecular docking with common pharmacophore matching, Journal of Medicinal Chemistry 51 (2008) 7882–7888.
[14] S.Y. Yang, Pharmacophore modeling and applications in drug discovery: challenges and recent advances, Drug Discovery Today 15 (2010) 444–450.
[15] R.A. Friesner, J.L. Banks, R.B. Murphy, T.A. Halgren, J.J. Klicic, D.T. Mainz, M.P. Repasky, E.H. Knoll, M. Shelley, J.K. Perry, D.E. Shaw, P. Francis, P.S. Shenkin, Glide: a new approach for rapid, accurate docking and scoring. 1. Method and assessment of docking accuracy, Journal of Medicinal Chemistry 47 (2004) 1739–1749.
[16] R.A. Friesner, R.B. Murphy, M.P. Repasky, L.L. Frye, J.R. Greenwood, T.A. Halgren, P.C. Sanschagrin, D.T. Mainz, Extra precision glide: docking and scoring incorporating a model of hydrophobic enclosure for protein–ligand complexes, Journal of Medicinal Chemistry 49 (2006) 6177–6196.
[17] T.A. Halgren, R.B. Murphy, R.A. Friesner, H.S. Beard, L.L. Frye, W.T. Pollard, J.L. Banks, Glide: a new approach for rapid, accurate docking and scoring. 2. Enrichment factors in database screening, Journal of Medicinal Chemistry 47 (2004) 1750–1759.
[18] D.S.G. Garrett, M. Morris, R.S. Halliday, H. Ruth, W.E. Hart, R.K. Belew, A.J. Olson, Automated docking using a Lamarckian genetic algorithm and an empirical binding free energy function, Journal of Computational Chemistry 19 (1999) 1639–1662.
[19] H. Soreq, S. Seidman, Acetylcholinesterase – new roles for an old actor, Nature Reviews Neuroscience 2 (2001) 294–302.
[20] F.J. Munoz, R. Aldunate, N.C. Inestrosa, Peripheral binding site is involved in the neurotrophic activity of acetylcholinesterase, Neuroreport 10 (1999) 3621–3625.
[21] M.F. Blasina, A.C. Faria, P.F. Gardino, J.N. Hokoc, O.M. Almeida, F.G. de Mello, C. Arruti, F. Dajas, Evidence for a noncholinergic function of acetylcholinesterase during development of chicken retina as shown by fasciculin, Cell and Tissue Research 299 (2000) 173–184.
[22] N.C. Inestrosa, J.P. Sagal, M. Colombres, Acetylcholinesterase interaction with Alzheimer amyloid beta, Sub-Cellular Biochemistry 38 (2005) 299–317.

[23] C.A. Lipinski, Drug-like properties and the causes of poor solubility and poor permeability, Journal of Pharmacological and Toxicological Methods 44 (2000) 235–249.
[24] M.L. Bolognesi, A. Cavalli, L. Valgimigli, M. Bartolini, M. Rosini, V. Andrisano, M. Recanatini, C. Melchiorre, Multi-target-directed drug design strategy: from a dual binding site acetylcholinesterase inhibitor to a trifunctional compound against Alzheimer's disease, Journal of Medicinal Chemistry 50 (2007) 6446–6449.
[25] P. Camps, X. Formosa, C. Galdeano, T. Gomez, D. Munoz-Torrero, M. Scarpellini, E. Viayna, A. Badia, M.V. Clos, A. Camins, M. Pallas, M. Bartolini, F. Mancini, V. Andrisano, J. Estelrich, M. Lizondo, A. Bidon-Chanal, F.J. Luque, Novel donepezil-based inhibitors of acetyl- and butyrylcholinesterase and acetylcholinesterase-induced beta-amyloid aggregation, Journal of Medicinal Chemistry 51 (2008) 3588–3598.
[26] S. Rizzo, C. Riviere, L. Piazzi, A. Bisi, S. Gobbi, M. Bartolini, V. Andrisano, F. Morroni, A. Tarozzi, J.P. Monti, A. Rampa, Benzofuran-based hybrid compounds for the inhibition of cholinesterase activity, beta amyloid aggregation, and abeta neurotoxicity, Journal of Medicinal Chemistry 51 (2008) 2883–2886.
[27] V. Tumiatti, A. Milelli, A. Minarini, M. Rosini, M.L. Bolognesi, M. Micco, V. Andrisano, M. Bartolini, F. Mancini, M. Recanatini, A. Cavalli, C. Melchiorre, Structure–activity relationships of acetylcholinesterase noncovalent inhibitors based on a polyamine backbone. 4. Further investigation on the inner spacer, Journal of Medicinal Chemistry 51 (2008) 7308–7312.
[28] A. Cavalli, M.L. Bolognesi, A. Minarini, M. Rosini, V. Tumiatti, M. Recanatini, C. Melchiorre, Multi-target-directed ligands to combat neurodegenerative diseases, Journal of Medicinal Chemistry 51 (2008) 347–372.
[29] M.I. Rodriguez-Franco, M.I. Fernandez-Bachiller, C. Perez, B. Hernandez-Ledesma, B. Bartolome, Novel tacrine-melatonin hybrids as dual-acting drugs for Alzheimer disease, with improved acetylcholinesterase inhibitory and antioxidant properties, Journal of Medicinal Chemistry 49 (2006) 459–462.
[30] J. Hardy, D.J. Selkoe, The amyloid hypothesis of Alzheimer's disease: progress and problems on the road to therapeutics, Science 297 (2002) 353–356.
[31] M.Y. Mizutani, A. Itai, Efficient method for high-throughput virtual screening based on flexible docking: discovery of novel acetylcholinesterase inhibitors, Journal of Medicinal Chemistry 47 (2004) 4818–4828.
[32] T.I. Oprea, H. Matter, Integrating virtual screening in lead discovery, Current Opinion in Chemical Biology 8 (2004) 349–358.